

Correlation effects and spin-orbit interactions in two-dimensional hexagonal $5d$ transition metal carbides, $\text{Ta}_{n+1}\text{C}_n$ ($n = 1, 2, 3$)

NINA J. LANE¹, MICHEL W. BARSOUM¹ and JAMES M. RONDINELLI¹ ^(a)

¹ *Department of Materials Science & Engineering, Drexel University, Philadelphia, PA 19104, USA*

PACS 73.63.-b – Low dimensional structures, electrical properties

PACS 73.22.-f – Electronic structure, condensed matter, nanoscale materials

Abstract – Density functional calculations are used to investigate the electronic structure of two-dimensional $5d$ tantalum carbides with honeycomb-like lattice structures. We focus on changes in the low-energy bands near the Fermi level with dimensionality. We find that the Ta $5d$ states dominate, and the extended nature of the wavefunctions makes them weakly correlated. The carbide sheets are prone to long range magnetic order and we evaluate their stability to enhanced electron–electron interactions through a Hubbard U correction. Lastly, we find that the splitting of the bands near the Fermi level caused by spin-orbit interaction decreases with increasing dimensionality. In the lowest dimensionality ($n = 1$) case, the band splitting pushes a conduction band above the Fermi level and leads to a semi-metallic band structure.

Two-dimensional (2D) free-standing crystals exhibit a range of functional properties, mainly derived from the topology of their underlying lattice and enhanced electronic and magnetic effects due to reduced dimensionality. Spin-polarized edge states, [?] for example, have been predicted for the well-studied 2D carbon material graphene, [?] owing to the topological origin of its transport properties. A large external magnetic field, however, is required to realize the quantum Hall effect, and its spin degeneracy makes it difficult to manipulate. To overcome these challenges, experimental approaches have been developed to induce magnetism by introducing transition metal adatoms [?] and point defects [?] on the surfaces.

2D binary metal oxides and dichalcogenides, e.g. ZnO, BN, MoS₂ also find widespread interest. New functionalities originate from the presence of more diverse chemistries. [?, ?] However, in most existing pristine 2D free standing materials, magnetic ordering is absent and the tunability of the electronic structure is limited to electrostatic doping. A more promising avenue includes directly incorporating transition metals with multiple orbital degrees of freedom and highly-correlated electrons into the lattice. Magnetism, for example, was recently predicted for VX₂ ($X = \text{S, Se}$) monolayers. [?] Alternatively, heavier $5d$ transition metals with strong spin-orbit coupling can be either deposited on the surface or directly integrated into the lattice of the 2D

materials. Recent first principles calculations show that graphene decorated with $5d$ transition metals can exhibit remarkable magnetic and topological transport properties [?]. The magnetic coupling induced by such treatments on nonmagnetic 2D materials, however, is difficult to control in actual applications due to unintentional impurities and defects.

In this Letter, we focus on low-dimensional hexagonal materials, consisting of alternating layers of carbon and tantalum. These Ta-containing transition metal carbides are part of a recently discovered group of 2D materials called “MXenes” synthesized by chemical exfoliation. [?] Similar to the previously studied Ta-decorated graphene structures, [?] these materials contain sheets of carbon in the inner layers and Ta atoms on the surface. In this case, however, the Ta layers are ordered, rendering them less susceptible to defects and more favorable for deliberate surface functionalization. Furthermore, these materials are derived from MAX phases, which are a large family of layered carbides and nitrides with the general formula $M_{n+1}AX_n$, where $n = 1 \cdots 3$, M is an early transition metal, A is an A-group element (mostly from groups 13 and 14), and X is carbon and/or nitrogen. [?] Since the stacking sequence of the XM_6 octahedra in the hexagonal MAX phases depends on the stoichiometry, the MXene sheets have the advantage that dimensionality controls both the system size and the symmetry between the two surfaces [Fig. 1(a)].

^(a)E-mail: jrondinelli@coe.drexel.edu

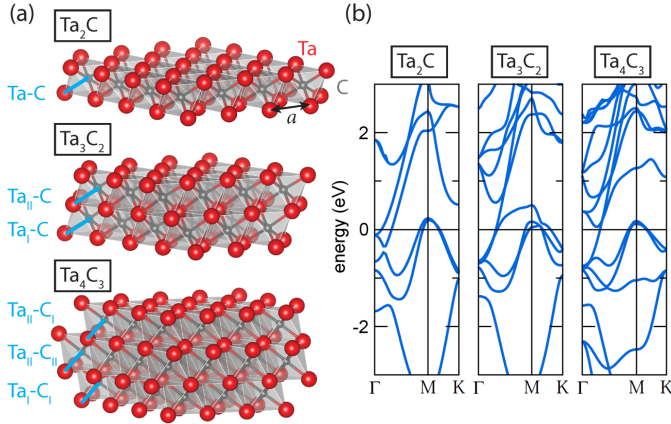


Fig. 1: The two-dimensional $\text{Ta}_{n+1}\text{C}_n$ ($n = 1, 2, 3$) sheets (a) all possess hexagonal symmetry. The lattice constants, a , and select interatomic Ta–C distances are highlighted (cf. Table 1). (b) LDA electronic band structures for each compound along the path $\Gamma(0, 0, 0) \rightarrow M(\frac{1}{2}, 0, 0) \rightarrow K(\frac{1}{2}, \frac{1}{2}, 0)$.

The 2D MXenes have the general formula $M_{n+1}X_n$, and they crystallize in sheets containing 1, 2, or 3 layers of XM_6 octahedra depending on n . Their recent synthesis [?] has spawned interest for uses in energy applications, including anodes in Li ion batteries [?, ?] and electrodes for supercapacitors. There are a number of recent theoretical studies, [?, ?, ?] mainly focusing on the Ti-containing phases. However, modeling work on MXenes in the Ta–C system have not yet been reported, despite their recent synthesis [?]. Motivated by the structural flexibility, possible enhanced electron–electron interactions, and the strong spin-orbit coupling parameter for Ta ($\zeta_d = 1970 \text{ cm}^{-1}$) [?], we use *ab initio* electronic structure calculations to investigate the effect of dimensionality (n) and electron correlations on the band structure and magnetic ordering in $\text{Ta}_{n+1}\text{C}_n$, $n = 1 \dots 3$.

First-principles density functional calculations are performed using the Vienna *Ab initio* Simulation Package (VASP) [?], with a plane wave cutoff of 500 eV and the projector-augmented wave method (PAW) [?] to treat the interaction between the core and valence electrons; we treat the Ta $5p$ electrons as valence electrons. For the site-decomposed density of states, partial occupations are set using the tetrahedron method with Blöchl corrections. In the band structure calculations, Gaussian smearing with a smearing width of 0.10 eV was used. Reciprocal space integrations are performed using a $15 \times 15 \times 2$ k -point mesh. We investigate the effects of electron–electron interactions by using both the local (spin) density approximation [L(S)DA] and the improved generalized gradient approximation (GGA) of Perdew-Burke-Eruzerhof (PBEsol) for solids [?] with the rotationally invariant Hubbard U correction (+ U) of Liechtenstein *et al.* [?]. **For the on-site exchange interaction, we test values of J from 0.2 to 1.5 eV and determine J does not have a strong effect on the stability of the magnetic configurations with U . J is therefore**

Table 1: Summary of lattice parameters, a , and Ta–C bond lengths, d , in Å with respect to dimensionality, n , obtained with LDA and PBEsol functionals. Embolden values correspond to experimental data taken from Ref. [?].

	n	length	LDA	PBEsol	
Ta ₂ C	1	a	3.041	3.058	
		$d(\text{Ta}-\text{C})$	2.127	2.139	
Ta ₃ C ₂	2	a	3.086	3.112	
		$d(\text{Ta}_{\text{I}}-\text{C})$	2.110	2.127	
		$d(\text{Ta}_{\text{II}}-\text{C})$	2.220	2.236	
Ta ₄ C ₃	3	a	3.077	3.094	(3.1)
		$d(\text{Ta}_{\text{I}}-\text{C})$	2.119	2.131	
		$d(\text{Ta}_{\text{II}}-\text{C}_{\text{I}})$	2.201	2.210	
		$d(\text{Ta}_{\text{II}}-\text{C}_{\text{II}})$	2.215	2.226	

kept constant at 0.5 eV throughout. The high measured conductivity of Ta₄C₃ [?], and the robustly metallic electronic structures of bulk TaC [?] and the MAX phases [?], suggest that electron correlation effects should be weak. We, therefore, anticipate the LDA and PBEsol functionals to provide an adequate description of the electronic and magnetic properties of these materials.

The $\text{Ta}_{n+1}\text{C}_n$ unit cells used in our calculations contain two symmetry equivalent free-standing sheets that are separated by 11–13 Å of vacuum. We obtain the equilibrium structures at the LDA and PBEsol level by minimization of the total energy computed for a range of a lattice parameters, performing a full relaxation of the atomic positions along the c -direction until the forces are converged below a tolerance of 5 meV Å⁻¹.

Table 1 contains the ground state atomic structure descriptors obtained with the LDA and PBEsol functionals. These ground state atomic structures are used for all subsequent band structure and energy calculations according to the corresponding dimensionality and functional. The LDA functional, for all values of n , predicts equilibrium lattice parameters that are smaller than those obtained with PBEsol; nonetheless, both functionals are in good agreement, within < 1% of each other and the available experimental data [?] for Ta₄C₃. We also summarize the interatomic distances between the different Ta and C atoms corresponding to the sites labeled in Fig. 1(a). For all 2D sheets explored, the Ta atoms at the surface layer have shorter Ta–C bonds than those in the center of the sheet, i.e. $d(\text{Ta}_{\text{I}}-\text{C}) < d(\text{Ta}_{\text{II}}-\text{C})$, which is also consistent with the bond lengths in MAX phases [?].

While there are slight differences in the lattice dimensions and atomic positions, the average interatomic distances and lattice parameters are similar between the three stoichiometries. This suggests that any differences in electronic structure should originate from either the stacking of the octahedra or the number of occupied Ta d bands available, which depends on the ratio of Ta to C atoms. To explore these possible differences, we begin by computing

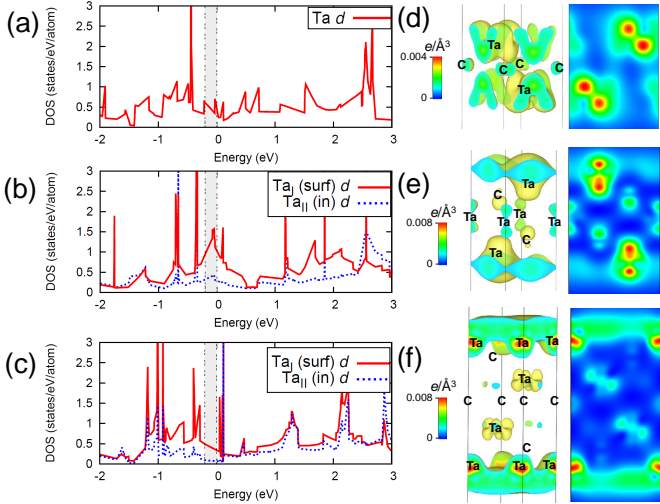


Fig. 2: Site-decomposed partial DOS computed within the LDA for the surface (surf) and inner (in) layer Ta sites in (a) Ta_2C , (b) Ta_3C_2 , and (c) Ta_4C_3 . Note that the contribution from the C atoms to the DOS within this energy window is small and therefore not shown. The spatial distribution of the partial charge density from 0.2 eV up to the Fermi level (shaded region) is also shown in (d), (e), and (f) for Ta_2C , Ta_3C_2 , and Ta_4C_3 , respectively. The 2D contours are projections on the $(11\bar{2}0)$ plane.

the electronic band structures with the LDA functional. For $n = 1$, we find two dispersive Ta d -bands crossing the Fermi level (E_F) along $\Gamma - \text{M}$ [Fig. 1(b), left]. The two free-electron pockets centered at Γ are similar to those found in 3D metals despite the 2D nature of the MXene sheet. Further, the hole pockets at M make this a semi-metal with possible p -type conductor features that may be highly temperature dependent.

In contrast, in Ta_3C_2 ($n = 2$) we find multiple bands crossings at the Fermi level, with metallic-like partial occupancy centered around M. The band structure for Ta_4C_3 ($n = 3$) shows similar features as Ta_2C , with nearly fully occupied Ta d states at M. However, in this case a single Ta band, with nearly linear dispersion, crosses the Fermi level along $\Gamma - \text{M}$. Indeed the site-decomposed partial densities-of-states (DOS) confirm that the region near E_F is largely controlled by the Ta d states [Figs. 2(a–c)].

Figs. 2(d–f) show the spatial distribution of the electrons within 0.2 eV of E_F . We find a strong dependence on dimensionality for the charge distribution. Intriguingly, this spatial distribution about the Ta site in $n = 1$, *viz* Ta_2C [Fig. 2(d)], and the inner Ta atom in $n = 3$, *viz* Ta_4C_3 [Fig. 2(f)], share similar features—the charge around the atom is distributed into six lobes, three above and three below the Ta atom. The inner Ta atom in $n = 2$ (Ta_3C_2) [Fig. 2(d)] shows strikingly different behavior, with a small distribution of charge collected above and below the Ta atom, aligned parallel to the c -axis.

To understand the atomic-scale origin of these features, we examine more closely the crystal structures of each sheet.

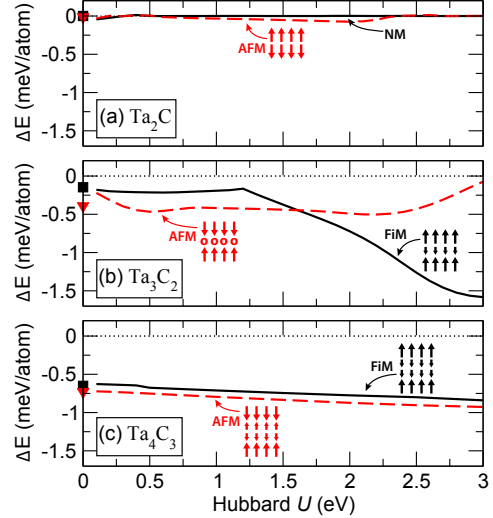


Fig. 3: The L(S)DA+ U energy differences, ΔE , between the magnetic and non-magnetic (NM) states with U for (a) Ta_2C , (b) Ta_3C_2 , and (c) Ta_4C_3 . Energies given per Ta atom. The points at $U = 0$ eV are obtained without the Hubbard U method. Schematics (inset) illustrate the spin ordering of the Ta atoms with ferrimagnetic (FiM) or antiferromagnetic (AFM) order, where the arrows represent the relative magnitudes and directions of spin, and the open circles indicate Ta atoms with no magnetic moment.

Ta_2C ($n = 1$) consists of a single Ta–C octahedron with stacking sequence AcB, where uppercase letters denote the Ta atom and lower case letters represent the stacking of carbon atoms. Ta_4C_3 ($n = 3$), therefore, is obtained as a Ta_2C layer, AcB, with an extra Ta atom on each surface – that is, Cb[AcB]aC. Note that this is the only structure in which two Ta atoms on either surface have the same stacking. On the other hand, Ta_3C_2 ($n = 2$) has a stacking sequence of AcBaC, so the symmetry of the AcB layer is broken due to the odd number of layers. This suggests that the differences in the charge distribution we find in Figs. 2(d–f) are largely governed by the stacking sequence of the CTa_6 units—a degree of freedom unique to the MXene phases. Such differences in the electron distribution near E_F due to the asymmetric stacking are also visible in the shape of the DOS [shaded region in Fig. 2(b)]. The charge is concentrated at the surface for Ta_3C_2 and Ta_4C_3 , consistent with the higher partial density of states for the Ta surface atoms [Figs. 2(b–c)].

The large number of Ta d -states at E_F and the sensitivity of the electronic structure to the sheet dimensionality suggest the possibility of stable long range magnetic spin configurations. We therefore performed a series of spin-polarized calculations with two different starting configurations, corresponding to ferromagnetic (FM), ferrimagnetic (FiM), and antiferromagnetic (AFM) spin order on the Ta sites to systematically explore the possible magnetic orders with respect to n . We carried out unconstrained-spin density calculations to find the stable magnetic ordering (Fig. 3) and compared the total energy of those states

Table 2: Summary of the stable spin polarized ground states for the $\text{Ta}_{n+1}\text{C}_n$ MXene phases using different exchange-correlation functionals with and without a Hubbard U correction. Notations (schematics) for the magnetic states are given in the caption (insets) to Fig. 3.

	Ta_2C	Ta_3C_2	Ta_4C_3
LDA	NM	AFM	AFM
LDA+U	AFM ($U > 0.5$)	FiM ($U > 1.6$)	AFM
PBEsol	AFM	AFM	NM
PBEsol+U	FM ($U > 0.1$)	FiM ($U > 0.9$)	NM

to that of the non-spin-polarized case. Given the limited ability of DFT to fully capture correlation effects, including transition metal ions with partially filled d shells, we now add the Hubbard U correction to the standard PBEsol (PBEsol+ U) and LSDA (LSDA+ U) functionals [?]. Since it was recently suggested that Ta-containing MAX phases are weakly correlated [?], we explored $U < 3.0$ eV.

Figure 3 shows the change in total energy of the spin-polarized states computed with the LSDA+ U functional compared to the non-magnetic (NM) case. The change in energy is calculated as a function of U by $\Delta E(U) = [E_M(U) - E_{NM}(U)]/N$, where $E_M(U)$ and $E_{NM}(U)$ are the total energies of the magnetic and non-magnetic states, respectively, for a given U value. N is the number of atoms per unit cell. In most cases, the magnetically ordered configurations are lower in energy than the NM state. For $n = 1$, the FM state could not be stabilized with LDA calculations, and weak magnetic ordering is observed in the metastable AFM state [Fig. 3(a)]. As the dimensionality increases, the AFM case becomes more stable. Our main results are summarized in Table 2, where the values in parentheses specify the U values above which the specific magnetic ordering becomes stable. For Ta_3C_2 , both LSDA+ U and PBEsol+ U calculations predict a FiM configuration, whereas an AFM ordering is predicted for Ta_4C_3 , but only with the LSDA+ U exchange-correlation functional (Table 2). Note that in Ta_4C_3 no ordered magnetic phase was found to be stable with either PBEsol and PBEsol+ U .

In all cases, the surface Ta atoms are spin polarized in the same direction for FiM order and in opposite directions for AFM. The Ta atoms in the inner layers are weakly spin-polarized in the direction opposite to the surface Ta atoms in both the FiM and AFM configurations, with the exception of the AFM configuration of Ta_3C_2 , which is constrained by symmetry. The addition of U generally has a small effect on the electronic structure, leading to a slight shift of the Ta d -bands uniformly to higher energies.

We now evaluate the effect of spin-orbit coupling (SOC) on the band structure with respect to n . Here we find that SOC splits the bands near the Fermi level, manifesting as a shift in energy, especially for the highest occupied Ta d -bands. It has the strongest effect on Ta_2C (Fig. 4), where the band splitting is prominent and pushes one of

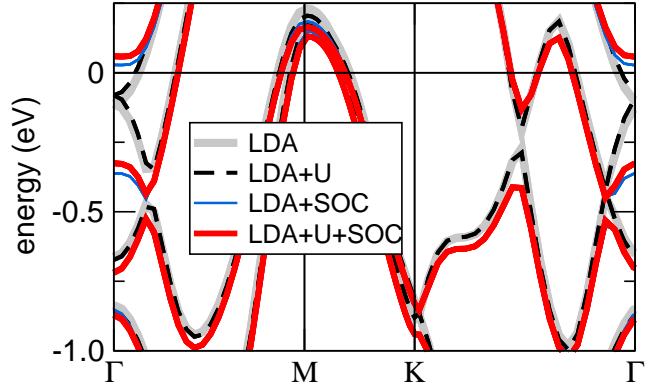


Fig. 4: LDA band structure for Ta_2C without spin or correlation (gray, thick lines), using LDA+ U with $U=1\text{eV}$ (black, broken lines), with spin-orbit coupling (SOC) (blue, solid lines), and with SOC using LDA+ U with $U=1$ eV (red, thick lines).

the formerly occupied degenerate bands below ≈ -0.11 eV to above E_F , driving a transition from a band structure with two band crossings to one with Fermi surface with small electron and hole pockets. Including electron correlation (+ U) within LDA and LDA+SOC causes only a small energy shift to those states (Fig. 4). For Ta_2C , the spin-orbit splitting at the top of the valence band at Γ ($\Delta_{SO}=269$ meV) is comparable to that observed in GaAs ($\Delta_{SO}=342$ meV) [?], and more than 3 orders of magnitude larger than graphene ($\Delta_{SO} \approx 0.05$ meV) [?]. The result is that this double band crossing near Γ shifts to a single linear band crossing as one band splits off and is pushed above the Fermi level. This shift toward a more semi-metallic electronic state should be experimentally observed in its transport properties, which are predicted to be fundamentally different from the $n = 2$ and $n = 3$ MXenes.

In summary, we have shown that the Ta-based $5d$ electronic structure is sensitive to dimensionality. All explored phases exhibit correlation stabilized magnetic order that is not found in the bulk MAX phase structures. The LSDA+ U method stabilizes the ferromagnetic ordering in the case of $n = 2$, and for $n = 1$ spin-orbit coupling shifts the electronic band structure with a transition from a two-band to a nearly filled single band. In these 2D MXenes, the electronic structure is controlled by the stacking of the CTa_6 octahedra and the states derived from the surface Ta atoms. Tailoring the electronic structure could therefore be achieved through end group functionalization of the surfaces of the MXene sheets. This opens up possibilities for engineering a class of tunable functional 2D materials. We conjecture that one could maintain a band structure with linear graphene-like crossings where the Fermi surface is nearly completely controlled by a single band – like that observed in Ta_2C – through epitaxial strain engineering. Overall, the Ta-containing graphene-like carbides show great promise as functional 2D materials that can be synthesized in different dimensionalities, leading to a range of stacking sequences and stoichiometries that offer a variety of electronic and magnetic behaviors.

* * *

N.J.L. and M.W.B. were supported by the Assistant Secretary for Energy Efficiency and Renewable Energy, Office of Vehicle Technologies of the U.S. DOE under Contract No. DE-AC02-05CH11231, Subcontract 6951370 under the Batteries for Advanced Transportation Technologies (BATT) Program. N.J.L. acknowledges financial support by the Integrated Graduate Education and Research Traineeship (IGERT) under NSF (DGE-0654313), and J.M.R. was supported by ARO (W911NF-12-1-0133). This work benefited from the XSEDE (NSF) and the Center for Nanoscale Materials (U.S. DOE-BES, under Contract No. DE-AC02-06CH11357) HPC resources.